Fuel, Vol. 208, 15 November 2017, Pp. 203-213
DOI:10.1016/j.fuel.2017.07.018

The Kinetics and Pore Structure of Sorbents during the Simultaneous Calcination/Sulfation of Limestone in CFB

Liang Chen[1], Chunbo Wang [1], Ziming Wang[1], Edward J. Anthony[2]*

[1]School of Energy and Power Engineering, North China Electric Power University, Baoding 071000, China

[2]Institute for Energy and Resource Technology, School of Energy, Environment and Agrifood, Cranfield University, Cranfield, Bedfordshire MK43 0AL, UK

*Corresponding author. E-mail address: b.j.anthony@cranfield.ac.uk.

Abstract: The interaction of calcination and sulfation in the simultaneous calcination/sulfation of limestone sorbent under circulating fluidized bed boiler conditions was studied. A specially designed constant-temperature reactor which can stop the reaction at a given time was employed. When limestone entered the furnace of mixed gases of CO_2, O_2, SO_2, etc., its weight went down first, then up, so there was a minimum weight point. The whole reaction period could be divided into two stages by this minimum weight point, named the weight-loss stage and the weight-growth stage, which were dominated by the calcination reaction and by the sulfation reaction, respectively. In the weight-loss stage, the sulfation reaction took place and $CaSO_4$ formed simultaneously together with limestone calcination as long as SO_2 was present. In the weight-growth stage, the sulfation ratio at 60 min in simultaneous calcination/sulfation is 30.7% higher than that in the sequential calcination then sulfation process. The weight loss rate of limestone calcined in the presence of SO_2 was lower than that without SO_2 present but the final weight was higher. The calcination of limestone was slowed by the presence of SO_2; a probable mechanism was proposed, namely that the $CaSO_4$ formed may fill or plug the pores in the CaO layer, and impede the transfer of CO_2 and, therefore, retard the calcination reaction. This mechanism was supported by the observation that the effective diffusion coefficient of CO_2 in CaO produced in the presence of SO_2 was reduced. The impeding effect increased with increasing SO_2 concentration (0-3000 ppm), while, when the particle size decreased from 0.4-0.45 mm to 0.2-0.25 mm, the calcination rate of limestone was higher, no matter whether there was SO_2 present or not. The impeding effect was less pronounced at 880°C than at 850°C. The reason for this appears to be the fact that there was less $CaSO_4$ formed at 880°C and, therefore, fewer pores of the particle were filled or plugged.

Keywords: Calcination; Sulfation; Simultaneous reaction; Limestone; Kinetics; CFB

Highlights

- A specially designed constant-temperature reactor was developed to study simultaneous calcination and sulfation
- This device can stop the calcination and sulphation reaction at any time to permit examination of the two simultaneously occurring processes
- An occlusion phenomenon was demonstrated whereby sulfation delayed the calcination process, significantly effecting the overall sulfation reaction
- Clear evidence of this phenomenon was provided by calculations of the effective diffusion coefficient of CO_2 in the presence of SO_2
- The impeding effect of sulfation was less pronounced at higher temperatures as the

sulfation process itself becomes less effective

1. Introduction

The circulating fluidized bed (CFB) boiler is widely adopted for the combustion of solid fuels like coal, petroleum coke and household waste. In CFBs, limestone is usually used as the in-situ desulfurization sorbent. To capture SO_2, limestone goes through both a calcination reaction and a sulfation reaction in the furnace, which can be described by the following global reactions:

$$CaCO_3 \rightarrow CaO + CO_2 \quad (1)$$

$$CaO + SO_2 + 1/2O_2 \rightarrow CaSO_4 \quad (2)$$

Given their great importance, the calcination and sulfation reactions of limestone have been investigated frequently over the past several decades [1-3].

The calcination of $CaCO_3$ is an endothermic reaction, and about 182.1 kJ heat is needed to calcine 1 mole $CaCO_3$ [1]. The decomposition temperature of $CaCO_3$ depends on the CO_2 partial pressure in the reaction atmosphere, and the equilibrium CO_2 partial pressure (P, atm.) at a given decomposition temperature (T, K) of limestone can be calculated by the formula of Baker [4]

$$\log P = 7.079 - \frac{8308}{T} \quad (3)$$

The calcination of $CaCO_3$ can be controlled by three steps [5]: heat transfer to the reaction surface, mass transfer of CO_2 through the CaO product layer, and the intrinsic chemical reaction. Which of these steps has the most pronounced effect on the reaction rate depends on factors like particle size, temperature, and reaction atmosphere.

Gallagher and Johnson [6] investigated the calcination of 30 μm $CaCO_3$ by thermogravimetric analysis (TGA) at 900-950°C in a CO_2 atmosphere, and found that the reaction rate was determined by heat transport. Caldwell et al. [7] came to the same conclusion in a study comparing the decomposition rate of 30 μm $CaCO_3$ in three different sweep gases (He, Ar and N_2) between 550-680°C. However, in a study using small limestone particles and high-speed sweep, Borgwardt [5] found that the limestone calcination reaction rate is independent of heat transfer, and shows an Arrhenius relationship to temperature. The calcination reaction activation energy is about 205 kJ/mol according to Borgwardt [5], which is close to the value (209.5 kJ/mol) obtained by Powell and Searcy [8] in a study calcining a thin calcite crystal in vacuum.

Particle size is another factor that will influence the calcination rate of limestone. The research of Borgwardt [5] found that when particle size increases in the range 1-90 μm, the calcination reaction rate decreased noticeably. Another conclusion of Borgwardt [5] is that the calcination reaction rate is proportional to the initial surface area of the particle. An investigation by Hu and Scaroni [9] indicated that for particles >20 μm and temperatures >1200°C, external heat transfer and pore diffusion of CO_2 are the major causes of reaction resistance, and for particles <10 μm and temperature <800°C, chemical kinetics is the rate-controlling step.

The calcination reaction rate can also be influenced by the CO_2 partial pressure at the reaction surface. The influence of CO_2 on calcination rate of $CaCO_3$ was investigated experimentally by Khinast et al.[10], who found that the reaction rate decreased exponentially with increasing CO_2 partial pressure. However, other studies found that the reaction rate was inversely proportional to CO_2 pressure or the difference between CO_2 pressure at the reaction surface and equilibrium

pressure [11, 12].

The sulfation reaction rate of CaO can also be influenced by three steps: mass transfer of SO_2 through pores to the inner surface of the particle, solid state diffusion of reactant through the compact $CaSO_4$ product layer, and the intrinsic sulfation reaction. Commonly, the sulfation reactions of CaO include two reaction stages, a fast reaction stage controlled by the intrinsic sulfation reaction, and a slow reaction stage controlled by the diffusion of reactant through the $CaSO_4$ layer.

The sulfation reaction rate can be influenced by several factors, like temperature, SO_2 concentration, particle size, etc. Many studies have shown that there is an optimum temperature for sulfur capture of CaO in CFBs, around 850°C [1]. Why there is an optimum temperature for sulfur capture of limestone in CFB is, however, not very clear at present. Particle size is one of the main factors which influence the sulfation rate of CaO significantly. Smaller sizes decrease the SO_2 gas transport resistance, and improve the SO_2 concentration levels seen in the inner part of the particle. The sulfation behavior of four particle sizes of limestone (158, 353, 632 and 1788 μm) was tested by Adánez et al. [13], and the results showed there was an increase of the sulfation rate with decreasing CaO particle size. A similar conclusion was drawn by Borgwardt [14] in a study on the sulfation of three sizes of CaO particles (96, 250 and 1300 μm). Although fine limestone particles have a high sulfation rate, an excess of fine particles in CFBs will decrease the sulfur capture efficiency because of their short residence time in the furnace. SO_2 concentration also influences the sulfation reaction rate, but the reaction order of SO_2 obtained by different researchers varies significantly. The study of Simons et al. [15] showed that the sulfation reaction of CaO is of the order of 1 for SO_2, but the experiments of Borgwardt et al. [16] indicated that the sulfation reaction rate is of the order of 0.64.

One other factor that affects the reactivity and utilization of CaO is its pore structure, including pore surface area, porosity and pore size distribution. Gullett and Bruce [17] investigated the sulfation behavior of CaO experiencing different sintering durations, and found that although sintering caused the coalescence of pores smaller than 7 nm and reduced pore surface area by a half, the sulfation behavior was not influenced significantly, which indicates that pores smaller than 7 nm are not crucial for the sulfation behavior of CaO. Ghosh-Dastidar et al. [18] found that the internal pore structures have a determining effect on the initial reactivity and the final utilization of CaO, but a high pore surface area cannot ensure a high sulfation reactivity and conversion. If the CaO particles contain an abundance of small pores, the sulfation reaction of the particle will cease prematurely because small pores are very susceptible to pore blockage and plugging. Interestingly, the study of Mahuli et al. [19] suggested that to improve the sulfation performance of CaO, not only the total pore surface and pore volume, but also the proportion of pores in the size range of 5-20 nm should be increased.

From the description above, in most of the studies, the calcination of limestone was carried out in N_2 or air, and then sulfation of the calcined CaO was studied. What is interesting and somewhat surprising is that few studies considered the influence of SO_2 on calcination of limestone. Under CFB conditions, limestone is calcined in flue gas produced by coal firing. In this case, there will be hundreds or thousands of ppm SO_2 in the flue gas. Therefore, a reasonable speculation is that the SO_2 will react simultaneously with a calcining limestone particle according to reaction (2). Hence, $CaSO_4$ will form in the particle, and the calcination of the particle will be affected by the formed $CaSO_4$ accordingly. Usually the decomposition of a limestone particle will proceed from

the particle surface to the interior. Pores will form in the CaO layer, and serve as the diffusion path for CO_2. When sulfation takes place in the CaO layer, the $CaSO_4$ formed will fill and narrow the pores, increase the CO_2 transfer resistance, and consequently slow down the calcination reaction. There are several reasons why one should consider this hypothesis.

First, because of the large limestone particle size (about 0.1-2.0 mm) and low combustion temperature (about 850˚C) in CFBs, the complete decomposition of limestone particles requires hundreds of seconds [20], and this duration is long enough for the generation of significant amounts of $CaSO_4$. The second reason is that the sulfation reaction of CaO is very fast in the initial reaction stage [21]. Considering the long decomposition duration and fast sulfation rate, the amount of $CaSO_4$ formed in the CaO layer may be considerable. Furthermore, the molar volume of $CaSO_4$ (46 cm^3/mol) is higher than that of both $CaCO_3$ (36.9 cm^3/mol) and CaO (16.9 cm^3/mol) [22], so the $CaSO_4$ formed will be dense and nonporous, and will occupy much of the pore space. When significant amounts of $CaSO_4$ form, the limestone particle pores will be narrowed or even blocked by $CaSO_4$, and as a result the calcination of limestone will be slowed or even stopped. If all the pores of the particle are plugged before the $CaCO_3$ is decomposed completely, some undecomposed $CaCO_3$ will be totally encompassed by the dense $CaSO_4$ layer, and can be expected to stay undecomposed in the following sulfation process. If this is the case, the calcination of limestone in the presence of SO_2 will be different from that in N_2 or air as usually practised in a TGA environment. This implies that the simultaneous calcination/sulfation reaction is the real reaction path in a CFB and should be studied rather than looking at sequential calcination and sulfation.

However, there is very little work that has paid attention to this issue. Keener et al. [23] investigated the simultaneous calcination and sulfation reactions with a structural pore model. They pointed out two effects of the calcination on the sulfation of limestone; one is the amount of surface area available for sulfation reaction, and the other, they noted, is that the mass transfer of SO_2 will be influenced by the transfer of CO_2. Unfortunately, the influence of the sulfation reaction on the calcination reaction of limestone was not further described. In a study by Alvfors and Svedberg [24], the partially-sintered spheres model was used to describe the simultaneous calcination and sulfation of limestone. And in yet another study, Mahuli et al. [25] studied the $CaCO_3$-SO_2 reaction with a grain-sub-grain model which considered the combined calcination, sintering, and sulfation reactions. Again, none of these studies described how sulfation will influence the calcination of limestone. A study by Olas et al. [26] on the mechanical activation of spent limestone from CFBs, found that $CaSO_4$ will immediately form on the surface of the particle when it is exposed to flue gas. Both the diffusion of SO_2 and CO_2 can then be limited by the $CaSO_4$ formed on the partially-calcined particle surface. However, no more details about the influence of sulfation on calcination were reported. Calcination was observed to be decayed by the sulfation reaction in the process of CO_2 capture by calcium-based sorbents in the presence of SO_2, according to the studies of Sun et al. [27, 28]. In summary, there is still very little real information on the true reaction process of limestone calcination and sulfation in CFBs currently available.

It is well recognized that one of the main problems in the field of CFBs is low calcium utilization in the SO_2 capture process by limestone. Although there have been hundreds of studies on this issue and many methods for the reactivation of limestone have been explored [29], this problem has not been adequately resolved. One of the most probable explanations is that most TGA and similar tests to realistically simulate the actual sulfation process, and hence the

experimental data are inconsistent with the real processes occurring in CFB boilers. According to this analysis simultaneous calcination/sulfation is a more realistic way to study limestone sulfation in CFBs, and this issue needs to be paid significantly more attention.

In our preliminary previous work [30, 31], the simultaneous calcination and sulfation of limestone in CFBs was investigated and from this work some important observations were made. First, the weight loss rate was slower for limestone calcined with SO_2; and second, some $CaCO_3$ was still undecomposed after 90 min of reaction [31]. However, two questions still remained: how the SO_2 influenced the calcination rate of limestone; and by what mechanism this influence occurs. The reason for these two questions being unresolved in our earlier work, was that a commercial TGA was used in that work [31]. Because in TGAs only the total weight of the sample can be obtained, the calcination rate cannot be measured separately from the test. The effect of SO_2 on calcination was hypothesized as masking the effect of formed $CaSO_4$ on the particle. This speculation should be verified by determining the difference between the CaO pore structure formed with and without SO_2. However, it is difficult to achieve this in a conventional TGA test. Since only10-mg or less samples can be collected from one TGA test, too many (about 100) repetitions are needed to collect enough samples (about 1g) for the pore-structure test.

To answer these questions, a specially designed experimental system (Fig. 1) was developed here. Unlike in the case of a TGA, the calcination ratio and sulfation ratio at a given time can be measured separately. Since about 50 mg of sample can be collected each time, it is practicable (20 repetitions needed) to collect enough samples for the pore-structure measurement. Based on this system, the interaction of calcination and sulfation reactions was tested, and the influence of SO_2 on the calcination reaction was properly explored for the first time. The effect of some factors, like temperature, SO_2 concentration, and particle size, were also determined. The pore volume and pore size distribution of CaO were measured, and the CO_2 diffusion coefficient in the pores was calculated to reveal the mechanism.

2. Experiments

Two types of limestone were tested, Baoding limestone and Xinxiang limestone. Prior to the test, both limestones were milled and sieved to two narrow particle size ranges (0.2-0.25 mm and 0.4-0.45 mm). The main components of the sorbents are listed in Table 1.

Table 1. Composition of limestones.

Compound (wt%)	SiO_2	Al_2O_3	Fe_2O_3	TiO_2	P_2O_5	CaO	MgO	SO_3	Na_2O	K_2O	Loss on Fusion
Baoding	0.67	0.78	<0.10	<0.05	<0.03	54.93	<0.10	<0.10	<0.10	<0.10	42.90
Xinxiang	0.45	0.56	0.15	0.05	<0.03	55.02	0.48	<0.10	<0.20	0.24	42.78

The limestone was calcined in a tube furnace, and its weight was measured and recorded continuously by a weight device connected to a computer, as shown in Fig. 1. The tube furnace is 40 mm ID by 800 mm length. The temperature in the furnace was monitored by an automatic controller (20-1200°C), with an accuracy of 2°C. The changes in sample weight were monitored every second by computer (the precision of the weight sensor is 0.1 mg). The reaction atmosphere was simulated by mixing N_2, O_2, CO_2, and SO_2 from gas cylinders.

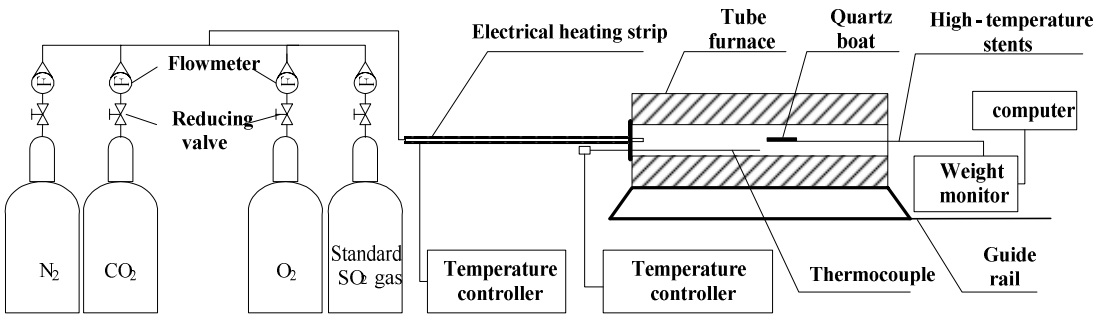

Fig. 1. The experimental system

All the experiments followed the same procedure. The tube furnace was first heated to the desired test temperature, and then the simulated flue gas was passed through the furnace for at least 10 min before the test was started. A given amount of sample (about 80±2 mg) was loaded into a quartz boat (100 mm long, 10 mm wide, and 5 mm deep) and moved into the furnace. Then the limestone was calcined and its weight was recorded continuously. The gas flow rate of 1.2 dm^3/min was used in all tests, and it was determined that this flow rate is high enough to eliminate the external gas diffusion resistance. Our previous work [32, 33] with this system showed it has sufficient accuracy for this type of study.

Since the limestone sample was calcined and sulfated simultaneously, the calcination ratio of the sample cannot be calculated from the weight data directly. To obtain the calcination ratio, the sample at a given reaction time was removed quickly from the furnace and cooled in N_2. Then the sample was weighed, crushed and calcined again in pure N_2, until the sample was calcined totally. And the calcination ratio of the sample was calculated by:

$$X_C = 1 - \frac{m_t}{\eta m_0}\frac{m_1 - m_2}{m_1}\frac{M_{CaCO_3}}{M_{CO_2}} \quad (4)$$

where m_0 is the initial sample weight; m_t is the sample weight after a given reaction duration; m_1 is the weight of sample after crushing; m_2 is the weight of the sample after being totally calcined; η is the $CaCO_3$ weight ratio of limestone, assuming that other impurities don't react; and M_{CaCO_3} and M_{CO_2} are the mole weight of $CaCO_3$ and CO_2, respectively. The sulfation ratio of the limestone samples can then be calculated by:

$$X_S = \frac{(1-x_t)\cdot\dfrac{m_t}{\eta m_0} + \dfrac{M_{CO_2}}{M_{CaCO_3}} - \dfrac{1}{\eta}}{\left(M_{CaSO_4} - M_{CaO}\right)\Big/ M_{CaCO_3}} \quad (5)$$

where x_t is the weight ratio of the undecomposed $CaCO_3$ in the sample; and M_{CaO} and M_{CaSO_4} are the molecular weights of CaO and $CaSO_4$, respectively.

All the tests were carried out at least three times to assure repeatability, and the error bars (standard deviation) have been shown in the figures. In all the tests based on duplicate runs the standard deviations of the calcination ratio were less than 1%. All the sample weight curves in the figures were normalized to initial sample weight of one unit (the normalized weight equals the sample weight divided by its initial weight). Table 2 summarizes the experimental conditions. The pore distribution of the calcined samples was measured by the N_2 adsorption/desorption method.

Table 2. Experimental conditions

conditions	value

Temperature (°C)	850, 880
CO_2 concentration (%)	15
O_2 concentration (%)	3
SO_2 concentration (ppm)	0, 1500,3000
N_2 concentration (%)	Balance
Particle size (mm)	0.2-0.25, 0.4-0.45

3. Results and Discussion

3.1. Simultaneous calcination/sulfation reaction

For convenience, results obtained when limestone was calcined in N_2 + 15% CO_2 and then sulfated, are designated as calcination-then-sulfation reaction. The differences between the simultaneous calcination/sulfation reaction and the calcination-then-sulfation reaction are shown in Fig. 2. In both cases 0.4-0.45 mm Baoding limestone was used, the temperature was 850°C and SO_2 was 3000 ppm.

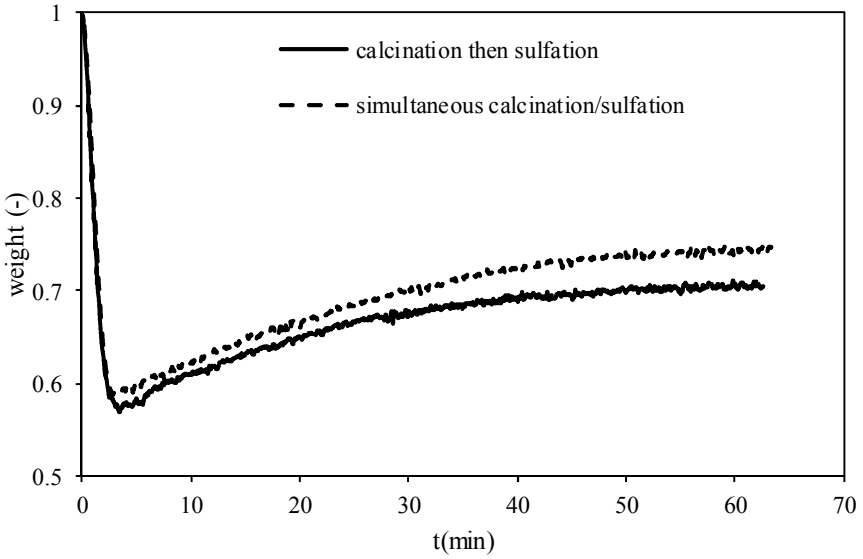

Fig. 2. Simultaneous calcination/sulfation compared with calcination-then-sulfation

As shown in Fig. 2, both curves displayed two stages with a minimum weight point. For discussion purposes, the two stages were named the weight-loss stage and the weight-growth stage, respectively. The minimum weight point of the calcination-then-sulfation curve was the end of the calcination and the start of the sulfation process, but this is not the case for the simultaneous calcination/sulfation reaction. Actually, the minimum weight point of the simultaneous calcination/sulfation curve was the point when the calcination rate was equal to the sulfation rate (by weight). Fig. 2 shows that the minimum weight points of the two reaction modes were different: 0.594 for the simultaneous calcination/sulfation curve; and 0.571 for the calcination-then-sulfation curve. The differences in the minimum weight and the weight-loss stage are discussed below.

For simultaneous calcination/sulfation, the calcination and sulfation reactions began once the sample was heated to the reaction temperature after reaching the furnace. The weight change of the sample was caused by the release of CO_2 in the calcination reaction and the capture of SO_2 in sulfation reaction. In the weight-loss stage, calcination was faster than sulfation (by weight), and

the reverse situation occurred in the weight-growth stage. After the minimum weight point, the calcination reaction continues, and its stopping point cannot be obtained from the curve. The calcination, however, can be stopped before completion. As indicated by the discussion above, some $CaCO_3$ may be covered in the core of the particle by $CaSO_4$, and remain undecomposed. However, if the $CaSO_4$ formation was not great enough, the calcination goes to completion. The way to test if the calcination is complete is evidently to measure the $CaCO_3$ in the sample.

In the weight-growth stage, some obvious differences between the two reaction modes can be found from Fig. 2. The weight of the sample in simultaneous calcination/sulfation was higher than that of the calcination-then-sulfation for the entire reaction duration. It seems that for the sulfation reaction the simultaneous calcination/sulfation mode is a better option than the calcination-then-sulfation approach. The weight-growth stage, which occurs due to the sulfation reaction, can be divided into two stages, a fast reaction stage (from the minimum weight point to 30 min) and a slow reaction stage (after 30 min). It can be seen from the figure that the difference between the two curves in the fast reaction stage changed very slightly (with weight difference being 4.0% at the minimum weight point to 3.5% at 30 min); but in the slow reaction stage, the weight-growth rate of the simultaneous calcination/sulfation reactions is faster than that of the calcination-then-sulfation reaction (with 5.8% weight difference at 60 min).

To calculate the sulfation ratio of the final sample in the simultaneous calcination/sulfation reaction, and determine whether there was undecomposed $CaCO_3$ in the sample, the samples must first be tested. Here, from the crushed and re-calcined sample at 850°C in N_2, the result showed no more weight loss, which means there was no more $CaCO_3$ in the sample. The sulfation ratio calculated by formula (5) was 17.9% for calcination-then-sulfation, and 23.4% for simultaneous calcination/sulfation, which is 30.7% higher than the former.

Based on Fig. 2, the approach to studying a sequential calcination-then-sulfation reaction for the simultaneous calcination/sulfation reaction will lead to significant errors. Since raw limestone is always used in CFBs, investigating simultaneous calcination/sulfation is the more accurate approach to studying the sulfation phenomena in CFB boilers.

The difference in the sulfation rates between the two reaction approaches should be due to the interaction of calcination and sulfation. The pore structures of samples at the minimum weight point can offer more information on the cause of these differences. Since the differences lie in the sulfation reaction occurring over the calcination stage, the investigation of the effect of SO_2 on calcination is necessary to better understand the real process.

3.2. Effect of SO_2 on Calcination of Limestone

3.2.1 Effect of SO_2 Concentration.

Here, Baoding limestone with particle size of 0.4-0.45 mm was tested first. The SO_2 concentration was 1500 ppm and 3000 ppm, and the temperature was 850°C. The calcination without SO_2 was also shown for comparison, in Fig. 3.

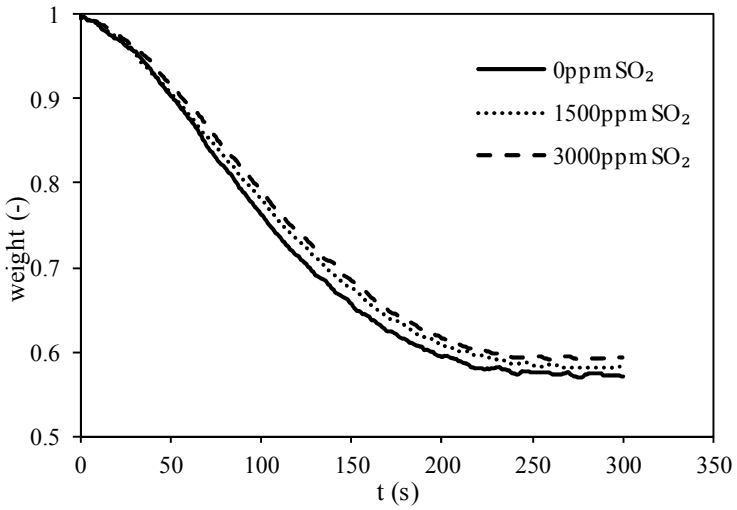

(a)

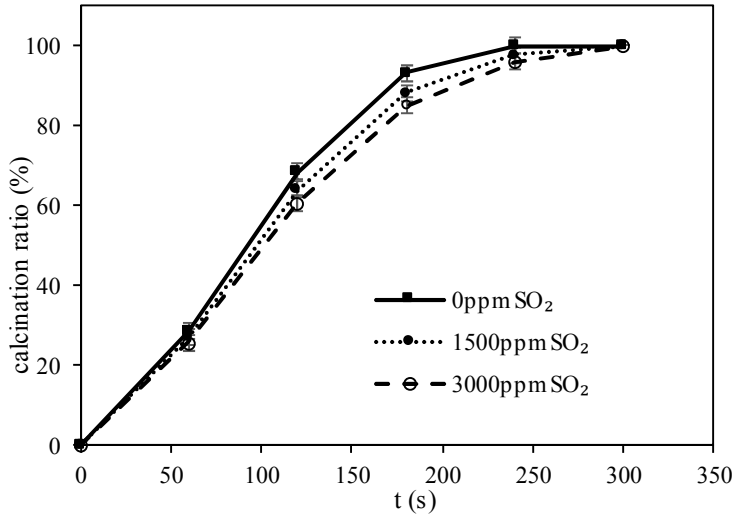

(b)

Fig. 3. Calcination of 0.4-0.45 mm Baoding limestone at 850°C with 3000 ppm or without SO_2. (a) the weight of samples; (b) the calcination ratio of samples.

First, consider the curves obtained under 0 and 3000 ppm SO_2 for discussion. As shown in Fig. 3(a), there are some obvious differences between the two curves. One is that the weight loss rate is significantly different. It is obvious that the weight loss rate of the sample without SO_2 was faster than that in the presence of 3000 ppm SO_2. Also, the final weight of the sample was different. The lowest weight (0.594) of the sample calcined with 3000 ppm SO_2 was about 4.0 % higher than that (0.571) of the sample calcined without SO_2. This observation was similar to that in our previous work obtained by TGA [31].

From Fig. 3(b), the influence of SO_2 on the calcination rate can also be observed. For example, the average calcination rate before 180 s in 3000 ppm SO_2 is 4.72×10^{-3}/s, which is 8.8% lower than that without SO_2 (5.17×10^{-3}/s). It seems clear that SO_2 had a retarding effect on the calcination of the sample.

Another thing that can be observed from Fig. 3(b) is that after 300 s of reaction, there was no more undecomposed $CaCO_3$ in the samples under all three conditions. However, in our previous work [31], there was 2-5% $CaCO_3$ left undecomposed in the final samples. This difference is

caused by the lower sulfation performance of the limestone used in this work. For a 60-min reaction, the sulfation ratio (about 35%) [31] of limestone used was much higher than that observed (about 23%) in this work. Given the lower sulfation ratio of limestone in this work, the $CaSO_4$ formed is less, and the pore filling effect of $CaSO_4$ on the particle is diminished, suggesting that some unplugged pores should remain until the complete decomposition of the limestone particles.

The influence of different SO_2 concentration can also be found in Fig. 3. The weight loss rate of the sample decreased with increased SO_2 concentration, as shown in Fig. 3(a), but the final weight increased. When the calcination atmosphere contained 1500 ppm and 3000 ppm SO_2, the final weight of the sample was 0.581 and 0.594, respectively, compared with the final weight 0.571 under conditions without SO_2. Since there was no more $CaCO_3$ in any of the final samples, a higher final weight indicated a higher sulfation ratio. And based on the same reaction time, it can be deduced that the sulfation rate increased with a raised SO_2 concentration. From Fig. 3(b), it can be seen that a different calcination rate of limestone was obtained under different SO_2 concentrations. The average calcination rate in 0-180 s under conditions with 0, 1500 and 3000 ppm SO_2 is 5.17×10^{-3}/s, 4.89×10^{-3}/s, and 4.72×10^{-3}/s, respectively. Thus, the conclusion to be drawn here is that more SO_2 in the reaction atmosphere will lead to a higher sulfation rate, and consequently decrease the calcination rate of limestone.

The influence of SO_2 on calcination of limestone acts by narrowing or blocking the pore in the CaO layer. When there is more SO_2 in the reaction atmosphere, the sulfation rate will be faster and more $CaSO_4$ will form in the pores of the CaO. In consequence, the CO_2 diffusion resistance will increase, but the calcination will be retarded. The influence of SO_2 on the pores is discussed in further detail below, based on the measurement of the pore structure.

Another limestone, Xinxiang limestone, was tested under the same conditions as that in Fig. 3 (850°C, 0.4-0.45 mm size). The weight change and calcination ratio results under SO_2 concentration of 0 or 3000 ppm are shown in Fig. 4.

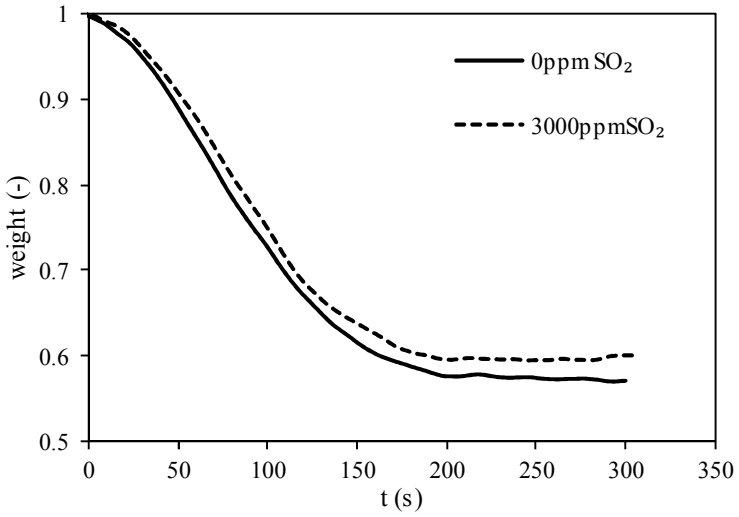

(a)

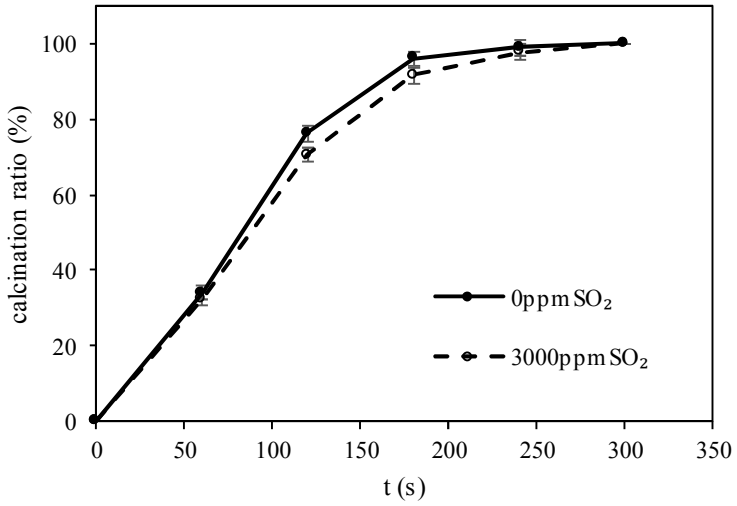

(b)

Fig. 4. Calcination of 0.4-0.45 mm Xinxiang limestone at 850°C with 3000 ppm or without SO_2. (a) the weight of samples; (b) the calcination ratio of samples.

The effect of SO_2 on calcination of Baoding limestone described above can also be found on Xinxiang limestone. For example, the final weight (0.601) of the sample calcined with 3000 ppm SO_2 was 5.4% higher than that (0.570) without SO_2; and the calcination rate was decreased by the presence of SO_2. So, the observations of Fig. 3 can be considered as a common phenomenon.

3.2.2 Effect of Temperature.

Under different temperatures, the influence extent of SO_2 on calcination of limestone may vary. Since CFBs usually operate at around 850-880°C, the temperatures 850°C and 880°C were chosen to test the effect of SO_2 under different temperatures, as in Fig. 5. The 0.4-0.45 mm Baoding limestone was used.

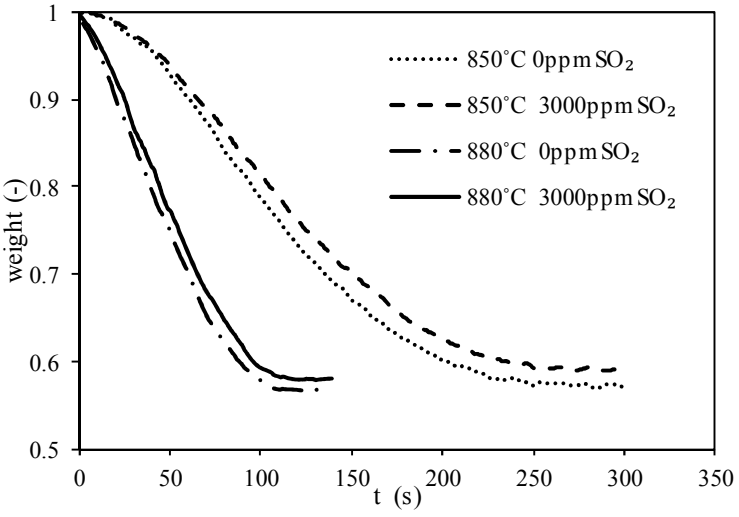

(a)

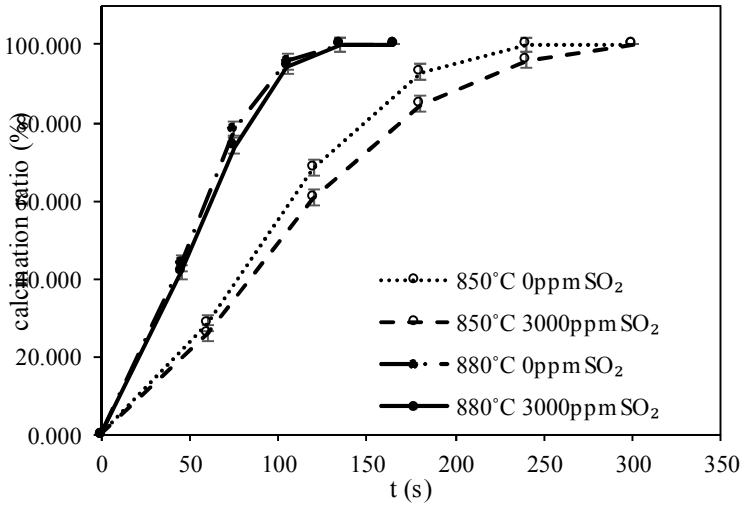

(b)

Fig. 5. Effect of temperature on the calcination of Baoding limestone. (a) the weight of samples; (b) the calcination ratio of samples.

As shown in Fig. 5(a), under the two temperatures tested, SO_2 had a strong influence on the calcination of limestone. Here, the two important influences of temperature on calcination are that the higher temperature had a remarkable effect on accelerating the calcination rate of limestone, regardless of whether there was SO_2 or not in the reaction atmosphere. Taking the condition without SO_2 for example, the average calcination rate at 880°C (7.69×10^{-3}/s) is about double that (3.85×10^{-3}/s) at 850°C. Another difference caused by temperature is that the final sample weight (0.594) with 3000 ppm SO_2 was higher at 850°C than that (0.580) at 880°C. Since limestone was calcined completely at 140 s under 880°C (Fig. 5(b)), the sulfation ratio of the final sample can be calculated by formula (5) with x_t=0. The calculated sulfation ratio (1.1 %) of the final sample at 880°C was lower than that (2.9%) at 850°C. The reduced (halved) reaction time appears to be the main reason for the low sulfation ratio at 880°C.

From Fig. 5(b), the impeding effect of SO_2 on calcination was more obvious at 850°C than 880°C. As discussed above, the influence of SO_2 on calcination appears to act through filling the pores in CaO by the formation of $CaSO_4$. Since the $CaSO_4$ formed was much less at 880°C, the filling effect of $CaSO_4$ was less than that at 850°C and, consequently, the impeding effect of SO_2 was also less pronounced at 880°C. The combined effect of temperature and SO_2 on the pore structure of CaO are explored in detail below by looking at the pore size distribution measurement.

3.2.3 Effect of Particle Size.

To study the effect of particle size on limestone calcination under conditions with SO_2, the 0.2-0.25 mm and 0.4-0.45 mm Baoding limestone was tested at 850°C, as shown in Fig. 6.

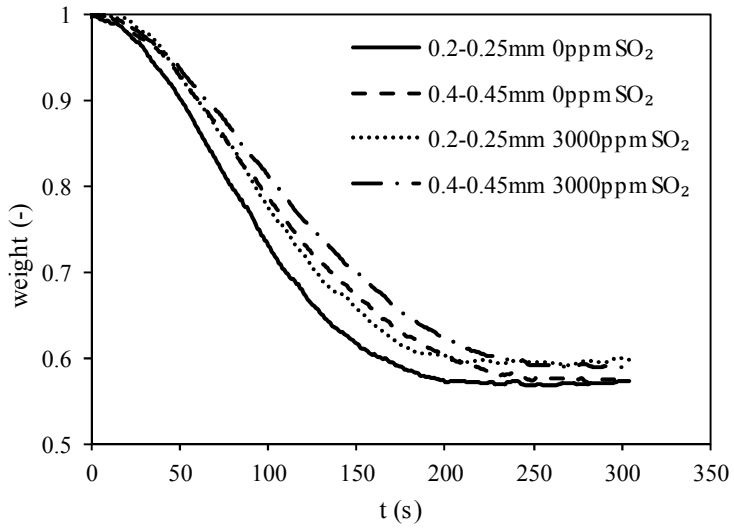

(a)

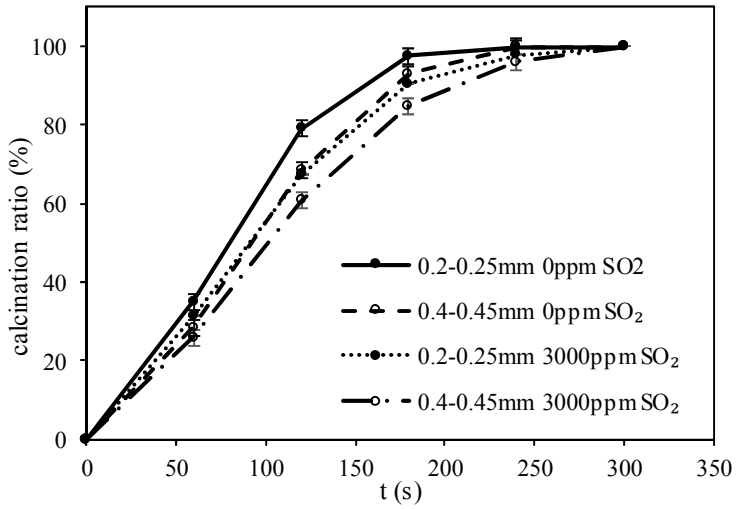

(b)

Fig. 6. Effect of particle size on the calcination of Baoding limestone. (a) the weight of samples; (b) the calcination ratio of samples

From the two curves without SO_2 in Fig. 6(a), it can be seen that the weight loss rate for the 0.2-0.25 mm particles is faster than that for the 0.4-0.45 mm particles. This means that there is an increase of the calcination rate with decreasing particle size, which can also be found in Fig. 6(b). For example, under conditions without SO_2, the calcination rate between 0-120 s is 6.6×10^{-3}/s for 0.2-0.25 mm particles, compared with 5.7×10^{-3}/s for the 0.4-0.45 mm particles. It can be inferred from the influence of particle size that the calcination reaction was partly controlled by the CO_2 diffusion resistance in the pores.

Under the influence of 3000 ppm SO_2, the weight loss rate of both particle sizes decreased; and from Fig. 6(b) it can be seen that the calcination rate also decreased. Smaller particles had a faster weight loss rate under the influence of 3000 ppm SO_2, as in Fig. 6(a). This shows that the changing particle size impacts more on the calcination rate (by weight) than on the sulfation rate (by weight) for the tested limestone. The final weight (0.599) of the 0.2-0.25 mm particles is 0.84% larger than that (0.594) of the 0.4-0.45 mm particles. Since the $CaCO_3$ in the particle was decomposed completely as shown in Fig. 6(b), the higher final weight of the smaller particles

demonstrates that its sulfation rate is higher than that for larger particles.

Although in our previous work the sulfation rate changed with particle size in the same way here, the weight loss rate changed in a different way—it decreased with a reduced particle size [31]. The sulfation of different limestone displayed a different sensitivity to particle size. For a limestone with high sulfation reactivity, its sulfation reaction will be more likely to be controlled by the SO_2 diffusion rate in the particle, and to be sensitive to the particle size change; for limestone with low sulfation reactivity this will not be the case [34]. The limestone used in the previous work had a higher reactivity and, so, its sulfation reaction was more sensitive to particle size. When the particle size decreased, its sulfation rate increased faster than calcination, and the weight loss rate decreased consequently. That appears to be the primary reason why its weight loss rate changed with particle size in an opposite way to that of this study.

3.3. Mechanism

3.3.1 Effect of SO_2 on Pore Structure of CaO

In the study by Blamey et al. [35, 36] on the calcination of $Ca(OH)_2$ under CO_2, it was found that an impermeable carbonate layer formed around the $Ca(OH)_2$ core, which can prevent CO_2 and H_2O diffusion. The decomposition of $Ca(OH)_2$ was stopped until the carbonate layer was ruptured by a high gas pressure in the closed pores within the particles. By analogy we can speculate that when calcining limestone particle in the presence of SO_2, $CaSO_4$ forms around the $CaCO_3$ core before $CaCO_3$ decomposes completely, the $CaSO_4$ layer can fill or seal the pores and thus slow down the calcination of $CaCO_3$ in a similar way.

Based on the analysis above to explain the effect of SO_2 seen in Fig. 3, the following mechanisms are proposed. For limestone calcined in an atmosphere without SO_2, the only reaction is the calcination of $CaCO_3$ (reaction (1)). But when limestone is calcined in an atmosphere containing SO_2, calcination and sulfation occur simultaneously in the particles. The sulfation reaction may influence the weight loss rate of the sample by two means. Thus, the sulfation reaction will increase the weight of CaO directly by the capture of SO_2. When limestone is calcined in an atmosphere containing SO_2, the change of the sample weight is the difference between the release of CO_2 and the absorption of SO_2. Under the tested conditions in this study, the sample weight declined with time. This illustrated that the weight loss rate caused by CO_2 release is faster than the weight gain rate caused by SO_2 capture.

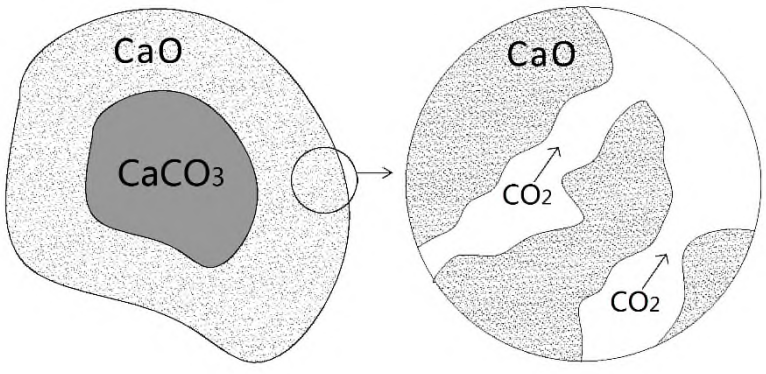

(a)

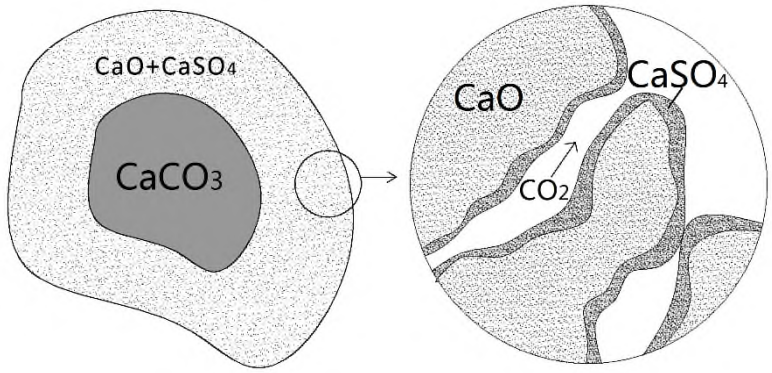

(b)

Fig. 7. Schematic of sulfation influence on the pore structure of limestone particle. (a) the calcination of limestone without SO_2; (b) the calcination of limestone with SO_2

Another way in which the sulfation reaction influences the weight loss rate is through slowing down the calcination reaction. The calcination reactions of limestone usually take place from the surface to the interior of the particles. Here, the pores formed in the CaO layer will serve as the diffusion path for CO_2, as in Fig. 7(a). But when the calcination atmosphere contains SO_2, the sulfation reaction will occur and $CaSO_4$ will form on the wall of the pores, as in Fig. 7(b). Because the molar volume of $CaSO_4$ is larger than that of $CaCO_3$ and CaO, the $CaSO_4$ layer formed will occupy more space in the pore. So the pore will be filled or blocked by $CaSO_4$, which will increase the CO_2 diffusion resistance out from the interior of the particle. The CO_2 partial pressure at the calcination surface will thus be improved. In this case, the calcination reaction rate will be decreased.

To prove the mechanisms put forward in Fig. 7, the 0.4-0.45 mm Baoding limestone calcined in 0/1500/3000 ppm SO_2 was collected. The Brunauer-Emmett-Teller (BET) surface area, pore volume and pore size distribution were measured. All the samples were collected at the minimum weight point. The results are shown in Table 3 and Fig. 8.

Table 3. Surface area and pore volume of CaO at 850°C.

SO_2 (ppm)	surface area (m^2/g)	pore volume (cm^3/g)
0	23.7	0.261
1500	18.7	0.239
3000	17.6	0.215

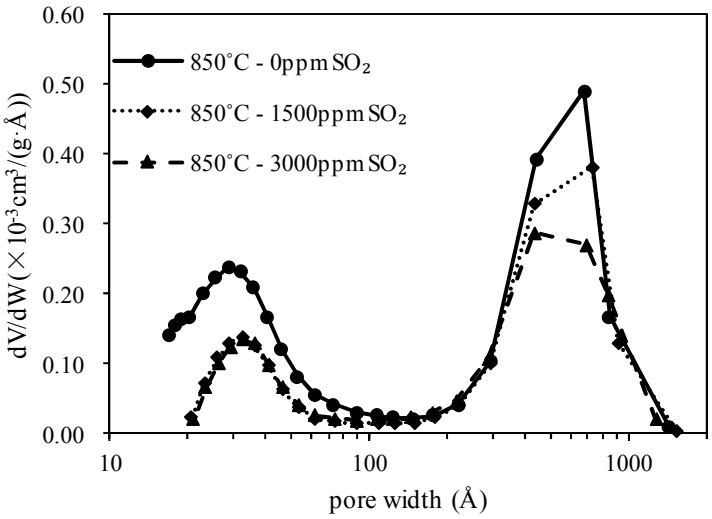

Fig. 8. The effect of sulfation on the pore size distribution

As shown in Fig. 8, the pore size is of bimodal distribution for each sample, with one peak at about 30 Å, and another at about 600 Å. The pores are mainly in the range 20-1500 Å, belonging to mesopore and macropore according to the classification of International Union of Pure and Applied Chemistry (IUPAC) [37].

The sulfation reaction has an obvious filling effect on the pores of CaO. Compared with the CaO formed without SO_2, both peaks of pore size distribution with 1500 ppm SO_2 were decreased significantly. As the SO_2 concentration increased to 3000 ppm, the peak at 600 Å was decreased further still. The pore structure change can also be observed from the BET surface area and pore volume given in Table 3. For example, the surface area and pore volume were decreased by 25.7% and 17.6%, respectively, for the CaO formed in 3000 ppm SO_2 compared with that without SO_2.

These pore structure variations indicated that during the calcination, the $CaSO_4$ formed filled the pores of the particles. However, with a higher SO_2 concentration, the filling effect will be more pronounced.

The pore structure variations will change the diffusion resistance of CO_2 in the pores. Diffusion through a porous particle can be calculated by Fick's first law:

$$Ns = -De\frac{d(C_{CO_2})}{d(l)} \quad (6)$$

where Ns is the diffusion flow rate of CO_2 in the radial direction through unit area, mol/(m^2s); De is the effective diffusion coefficient, m^2/s; C_{CO_2} is the concentration of CO_2, mol/m^3; and l is the diffusion distance. De mainly depends on the pore structure, and can be calculated by [38]:

$$De = D_A\varepsilon^2 \quad (7)$$

in which ε is porosity; and D_A is the diffusion coefficient in pore, m^2/s; D_A includes two patterns of diffusion, molecular diffusion and Knudsen diffusion, and

$$\frac{1}{D_A} = \frac{1}{D_{AB}} + \frac{1}{D_k} \quad (8)$$

where the molecular diffusion coefficient of CO_2 in N_2, D_{AB}, can be calculated by Fuller's formula [39]:

$$D_{AB} = \frac{1\times10^{-3}T^{1.75}(1/M_{N_2} + 1/M_{CO_2})^{0.5}}{p[(\sum_{N_2} v_i)^{1/3} + (\sum_{CO_2} v_i)^{1/3}]^2} \quad (9)$$

in which T is the reaction temperature, K; M_{N_2}, M_{CO_2} are the molar masses of N_2 and CO_2, respectively, g/mol; p is the total gas pressure, 1 atm; $\sum_{N_2} v_i$ and $\sum_{CO_2} v_i$ are diffusion volumes of N_2 and CO_2, which can be found elsewhere [39]. At 850°C (T = 1123K), and D_{AB} = 1.68 cm^2/s.

The Knudsen diffusion coefficient is:

$$D_k = \frac{97\bar{d}}{2}\sqrt{\frac{T}{M_{CO_2}}} \quad (10)$$

where $\bar{d}$ is average pore diameter, m. Assuming the pore is cylindrical, the average pore diameter can be calculated by:

$$\bar{d} = \frac{4V}{S} \quad (11)$$

where V is the pore volume, m^3/g; and S is the pore surface area, m^2/g. Formula (11) can only be used to calculate the average pore diameter of pores of unimodal distribution, and for pores of bimodal distribution, such as in Fig. 8, the best way to deal with the average pore diameter is to calculate the average diameter of each peak. As in Fig. 8, the pore of diameter around 100-200 Å is the lowest, and the distribution can be divided at 200 Å into two parts. The pore volume and surface area of pores smaller and larger than 200 Å can be obtained from N_2 adsorption. The calculated D_k, D_A and De are shown in Table 4.

Table 4. The diffusion coefficients

pore width	<200 Å			>200 Å		
SO_2 (ppm)	0	1500	3000	0	1500	3000
$\bar{d}$/(Å)	42.0	49.9	54.2	555.8	557.2	556.9
ε	0.019	0.011	0.013	0.444	0.431	0.403
D_k ($10^{-2}cm^2/s$)	1.030	1.224	1.327	13.62	13.65	13.65
D_A ($10^{-2}cm^2/s$)	1.023	1.215	1.317	12.60	12.62	12.62
De ($10^{-6}cm^2/s$)	3.825	1.404	2.099	24878	23474	20532

From Table 4, the diffusion coefficients in pores, D_A, are all close to D_k, and far smaller than D_{AB}, which means that the main diffusion pattern in the pores is Knudsen diffusion. The effective diffusion coefficients, De, of pores <200 Å are far smaller than those of pores >200 Å, so the contribution of pores <200 Å to gas diffusion can be ignored. And for pores >200 Å, De of samples generated in 1500 ppm and 3000 ppm SO_2 are 5.6% and 17.5% smaller, respectively, than those without SO_2. The decrease in De means an increase of the diffusion resistance, and a slower diffusion flow based on formula (6), which will increase the CO_2 concentration at the calcination reaction surface, and consequently decrease the calcination reaction.

The effectiveness factor can be used to assess the effect of diffusion on the reaction rate quantitatively. According to Ishida and Wen [40], the effectiveness factor η for the calcination reaction can be calculated by

$$\eta = \frac{3}{\phi}\left[\coth(\phi) - \frac{1}{\phi}\right] \quad (12)$$

where $\phi = R\sqrt{k_v / D_e}$ is the Thiele modulus, in which R is the radius of the particle, k_v is the reaction rate constant per unit volume, 1/s. The k_v can be calculated from the rate equation

$$r_c = k_v(C^e_{CO_2} - C_{CO_2}) \qquad (13)$$

where r_c is the calcination rate per unit volume limestone particles, mol/(m^3·s), and can be obtained from Fig. 3 under the assumption that the calcination is controlled by the intrinsic reaction. $C^e_{CO_2}$ is the equilibrium concentration of CO_2 for the calcination of limestone, which can be calculated from formula (3). C_{CO_2} is the CO_2 concentration in the reaction atmosphere, mol/m^3.

The calculated effectiveness factors for calcination of Baoding 0.4-0.45 mm particles at 850°C under 0, 1500, and 3000 ppm SO_2 are 0.823, 0.815 and 0.796, respectively. First, the effectiveness factors are far less than 1, which means that the diffusion in the pores clearly impeded the reaction. Second, with more SO_2 in the calcination atmosphere, the effectiveness factor decreased. This illustrated that the formed $CaSO_4$ increased the resistance of diffusion on the calcination rate, which is consistent with the findings in Fig. 3.

Through a similar process, the effectiveness factor can be calculated for the sulfation reaction after the calcination is complete, based on Fig. 2. The effectiveness factors are 0.580 for sulfation of 0.4-0.45 mm Baoding limestone in simultaneous calcination/sulfation, and 0.615 for the sulfation of CaO. This means that the sulfation reactions under the two conditions here are controlled by both the intrinsic reaction and diffusion in the pores.

3.3.2 Combined Effect of Sintering and SO_2 on the Pore Structure of CaO.

As discussed in section 3.2.2, the reduced impeding effect at higher temperature was attributed to a smaller number of filled pores. To test this explanation, the calcined sample of Baoding 0.4-0.45 mm limestone at 880°C with or without SO_2 were collected and measured by the N_2 adsorption/desorption method. All samples were collected at the minimum weight point. The measured surface area and pore size distribution are shown in Table 5 and Fig. 9, and for comparison the pore structure of samples at 850°C are also presented.

Table 5. Surface area and pore volume of CaO

temperature(°C)	SO_2 (ppm)	surface area (m^2/g)	pore volume (cm^3/g)
850	0	23.7	0.261
850	3000	17.6	0.215
880	0	21.1	0.248
880	3000	19.6	0.234

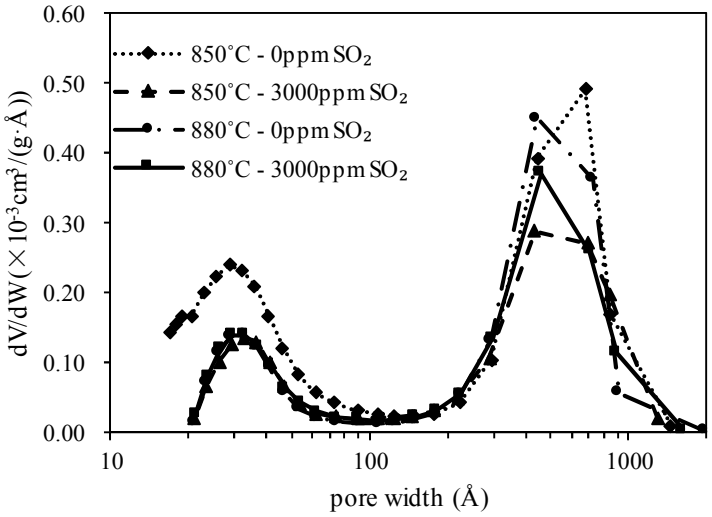

Fig. 9. The effect of temperature and SO_2 on the pore size distribution

As shown in Fig. 9, the pore-size curves at 880°C show bimodal distribution similar to results observed at 850°C. But compared with those without SO_2, the pore-size distribution with 3000 ppm SO_2 at 880°C shows an obvious decline. So, the filling effect of $CaSO_4$ is still obvious at 880°C.

Some transformation of the pores occurs when temperature is increased. Taking the two curves without SO_2 in Fig. 9, for example, both peaks of the curve were lowered at 880°C. This means the volume of both mesopores and macropores were decreased. Since there was no SO_2 in the calcination stage of these two samples, the transformation was caused by an accelerated CaO sintering due to the raised temperature. The sintering effect of temperature can also be obtained from the pore structure data of Table 5. Considering the CaO formed without SO_2, for example, the surface area and pore volume at 880°C were decreased by 11.0% and 5.0%, respectively, compared to those at 850°C.

As discussed in section 3.2.2, it is hypothesized that the filling effect of $CaSO_4$ was less significant at 880°C. This speculation can be supported by the data of Fig. 9 and Table 5. As shown in Fig. 9, the difference between the pore-size-distribution peak values with and without SO_2 was smaller at 880°C than at 850°C. This means the pore volume filled or plugged was less at 880°C. While from Table 4, it can be seen that the decline of the pore volume (0.014 cm^3/g) caused by sulfation at 880°C was only 30% of that (0.046 cm^3/g) at 850°C. A smaller pore volume filled will provide a wider gas passage, and decrease the CO_2 diffusion resistance. In consequence, the impeding effect of $CaSO_4$ on calcination will be less pronounced.

Another interesting phenomenon can also be observed from the data in Table 5—the pore volume (0.234 cm^3/g) of CaO generated in 3000 ppm SO_2 and 880°C was larger than that (0.215 cm^3/g) at 850°C. Also, the surface area changed in the same manner, which is opposite to the situation observed without SO_2. It seems that the sulfation reaction influenced the pore surface area and pore volume more significantly than sintering did when temperature increased from 850°C to 880°C for the tested limestone.

4. Conclusions

The interactions between calcination and sulfation of limestone under CFB conditions were studied. The sulfation ratio at 60 min in simultaneous calcination/sulfation is 30.7% higher than

that in the calcination-then-sulfation reaction. Sulfation reactions occur and $CaSO_4$ is formed simultaneously with limestone calcination while SO_2 is present. The weight loss rate of the calcining limestone in the presence of SO_2 was lower than that without SO_2, but the final weight was higher. The calcination of limestone was impeded by the presence of SO_2, and the impeding effect was enhanced with increasing SO_2 concentration (0-3000 ppm). From these results a mechanism based on pore structure variation of CaO is proposed. The $CaSO_4$ formed fills or plugs the pore in the CaO layer, impeding the transfer of CO_2 and, therefore, retarding the calcination reaction. This mechanism was demonstrated by the reduced diffusion coefficient of CaO generated with SO_2. When particle size decreased from 0.4-0.45 mm to 0.2-0.25 mm, the calcination rate of limestone was higher, no matter whether there was SO_2 present or not. The impeding effect was less pronounced at 880°C than at 850°C. This may be explained by the smaller amount of $CaSO_4$ formed and thus reduced filling or plugging of pores in the particle at 880°C. In the presence of 3000 ppm SO_2 and with temperature increased from 850°C to 880°C, the sulfation reaction, rather than sintering, had a more significant effect on the pore structure of CaO.

Acknowledgement

This work was supported by the National Key Research and Development Program of China [2016YFB0600701]; the Fundamental Research Funds for the Central Universities [2016XS105].

References

[1] Anthony EJ, Granatstein DL. Sulfation phenomena in fluidized bed combustion systems. *Progress in Energy and Combustion Science* **2001**;27(2):215-236.

[2] Ar İ, Doğu G. Calcination kinetics of high purity limestones. *Chemical Engineering Journal* **2001**;83(2):131-137.

[3] Wu Y, Wang C, Tan Y, Jia L, Anthony EJ. Characterization of ashes from a 100kWth pilot-scale circulating fluidized bed with oxy-fuel combustion. *Applied Energy* **2011**;88(9):2940-2948.

[4] Baker EH. Calcium Oxide-Carbon dioxide System in the Pressure Range 1-300 Atmospheres. *Journal of the Chemical Society* **1962**;70:464-470.

[5] Borgwardt RH. Calcination Kinetics and Surface Area of Dispersed Limestone Particles. *AIChE Journal* **1985**;31(1):103-111.

[6] Gallagher PK, Johnson Jr DW. The effects of sample size and heating rate on the kinetics of the thermal decomposition of $CaCO_3$. *Thermochimica Acta* **1976**;6(1):67-83.

[7] Caldwell KM, Gallagher PK, Johnson Jr DW. Effect of thermal transport mechanisms on the thermal decomposition of $CaCO_3$. *Thermochimica Acta* **1977**;18(1):15-19.

[8] Powell EK, Searcy AW. The Rate and Activation Enthalpy of Decomposition of $CaCO_3$. *Metallurgical Transactions B* **1980**;11B:427-432.

[9] Hu N, Scaroni AW. Calcination of pulverized limestone particles under furnace injection conditions. *Fuel* **1996**;75(2):177-186.

[10] Khinast J, Krammer GF, Brunner C, Staudinger G. Decomposition of limestone: The influence of CO_2 and particle size on the reaction rate. *Chemical Engineering Science* **1996**;51(4):623-634.

[11] Ingraham TR, Marier P. Kinetic Studies on the Thermal Decomposition of Calcium

Carbonate. *The Canadian Journal of Chemical Engineering* **1963**;41(4):170-173.
[12] Darroudi T, Searcy AW. Effect of CO_2 pressure on the rate of decomposition of calcite. *The Journal of Physical Chemistry* **1981**;85(26):3971-3974.
[13] Adánez J, Labiano FG, Abánades JC, Diego LFD. Methods for characterization used in fluidized bed boilers of sorbents. *Fuel* **1994**;73(1):355-362.
[14] Borgwardt RH. Kinetics of the Reaction of SO_2 with Calcined Limestone. *Environmental Science & Technology* **1970**;4(1):59-63.
[15] Simons GA, Garman AR, Boni AA. The Kinetic Rate of SO_2 Sorption by CaO. *AIChE Journal* **1987**;33(2):211-217.
[16] Borgwardt RH, Bruce KR, Blake J. An Investigation of Product-Layer Diffusivity for CaO Sulfation. *Industrial & Engineering Chemistry Research* **1987**;26(10):1993-1998.
[17] Gullett BK, Bruce KR. Pore distribution changes of calcium-based sorbents reacting with sulfur dioxide. *AIChE Journal* **1987**;33(10):1719-1726.
[18] Ghosh-Dastidar A, Mahuli SK, Agnihotri R, Fan LS. Ultrafast Calcination and Sintering of $Ca(OH)_2$ Powder: Experimental and Modeling. *Chemical Engineering Science* **1995**;50(13):2029-2040.
[19] Mahuli SK, Agnihotri R, Chauk S, Ghosh-Dastidar A, Wei S, Fan L. Pore-structure optimization of calcium carbonate for enhanced sulfation. *AIChE Journal* **1997**;43(9):2323-2335.
[20] Dam-Johansen K, Østergaard K. High-temperature reaction between sulphur dioxide and limestone—I. Comparison of limestones in two laboratory reactors and a pilot plant. *Chemical Engineering Science* **1991**;46(3):827-837.
[21] Borgwardt RH, Bruce KR. Effect of Specific Surface Area on the Reactivity of CaO with SO_2. *AIChE Journal* **1986**;32(2):239-246.
[22] Dam-Johansen K, Østergaard K. High-temperature reaction between sulphur dioxide and limestone—II. An improved experimental basis for a mathematical model. *Chemical Engineering Science* **1991**;46(3):839-845.
[23] Keener SU, Khang SJ, Keener TC. A Calcination and Sulfation Reaction Model for Calcium Carbonate with Sulfure Dioxide. *Advances in Environmental Research* **1998**;2(3):251-268.
[24] Alvfors P, Svedberg G. Modelling of the simultaneous calcination, sintering and sulfation of limestone and dolomite. *Chemical Engineering Science* **1992**;47(8):1903-1912.
[25] Mahuli SK, Agnihotri R, Jadhav R, Chauk S, Fan L. Combined Calcination, Sintering and Sulfation Model for $CaCO_3$-SO_2 Reaction. *AIChE Journal* **1999**;45(2):367-382.
[26] Olas M, Kobyłecki R, Bis Z. Simultaneous calcination and sulfation of limestone-based sorbents in CFBC - Effect of mechanical activation. Proceedings of the 9th international conference on circulating fluidized beds, in conjunction with the 4th international VGB workshop "operating experience with fluidized bed firing systems", Hamburg, Germany; May 13-16, 2008: 931-936.
[27] Sun P, Grace JR, Lim CJ, Anthony EJ. Simultaneous CO_2 and SO_2 Capture at Fluidized Bed Combustion Temperatures. 18th International Conference on Fluidized Bed Combustion, Toronto, Ontario, Canada; 2005: 1-17.
[28] Sun P, Grace JR, Lim CJ, Anthony EJ. Removal of CO_2 by Calcium-Based Sorbents in the Presence of SO_2. *Energy & Fuels* **2007**;21(1):163-170.
[29] Anthony EJ, Bulewicz EM, Jia L. Reactivation of limestone sorbents in FBC for SO_2 capture.

Progress in Energy and Combustion Science **2007**;33(2):171-210.

[30] Wang C, Chen L. The effect of steam on simultaneous calcination and sulfation of limestone in CFBB. *Fuel* **2016**;175:164-171.

[31] Wang C, Chen L, Jia L, Tan Y. Simultaneous calcination and sulfation of limestone in CFBB. *Applied Energy* **2015**;155:478-484.

[32] Wang C, Zhang Y, Jia L, Tan Y. Effect of water vapor on the pore structure and sulfation of CaO. *Fuel* **2014**;130:60-65.

[33] Wang C, Zhou X, Jia L, Tan Y. Sintering of Limestone in Calcination/Carbonation Cycles. *Industrial & Engineering Chemistry Research* **2014**;53(42):16235-16244.

[34] Borgwardt RH, Harvey RD. Properties of Carbonate Rocks Related to SO_2 Reactivity. *Environmental Science & Technology* **1972**;6(4):350-360.

[35] Blamey J, Lu DY, Fennell PS, Anthony EJ. Reactivation of CaO-Based Sorbents for CO_2 Capture: Mechanism for the Carbonation of $Ca(OH)_2$. *Industrial & Engineering Chemistry Research* **2011**;50(17):10329-10334.

[36] Blamey J, Manovic V, Anthony EJ, Dugwell DR, Fennell PS. On steam hydration of CaO-based sorbent cycled for CO_2 capture. *Fuel* **2015**;150:269-277.

[37] Sing KSW, Everett DH, Haul RAW, Moscou L, Pierotti RA, J R, et al. Reporting physisorption data for gas/solid systems with special reference to the determination of surface area and porosity (Recommendations 1984). *Pure and Applied Chemistry* **1985**;57(4):603-619.

[38] García-Labiano F, Abad A, De Diego LF, Gayán P, Adánez J. Calcination of calcium-based sorbents at pressure in a broad range of CO_2 concentrations. *Chemical Engineering Science* **2002**;57(13):2381-2393.

[39] Fuller EN, Schettler PD, Giddings JC. New Method for Predition of Binary Gas-phase Diffusion Coefficients. *Industrial & Engineering Chemistry* **1966**;58(5):18-27.

[40] Ishida M, Wen CY. Comparison of Kinetic and Diffusional Models for Solid-Gas Reactions. *AIChE Journal* **1968**;14(2):311-317.

2017-07-14

The kinetics and pore structure of sorbents during the simultaneous calcination/sulfation of limestone in CFB

Chen, Liang

Elsevier

Liang Chen, Chunbo Wang, Ziming Wang, Edward J. Anthony, The kinetics and pore structure of sorbents during the simultaneous calcination/sulfation of limestone in CFB, Fuel, Volume 208, 15 November 2017, Pages 203-213

http://dx.doi.org/10.1016/j.fuel.2017.07.018